talenta PUBLISHER

Eco Chemical Engineering Journal

Journal homepage: https://talenta.usu.ac.id/EcoChe

Integrated Aspen Plus Simulation of Biogas Upgrading and Electricity Generation from Palm Oil Mill Effluent

Suratni Afrianti*[1], Andry Admaja Tarigan[1], Taufiq bin Nur[2]
[1]Department of Agrotechnology, Faculty of Agriculture, Universitas Prima Indonesia, Medan 20111, Indonesia
[2]Department of Mechanical Engineering, Universitas Sumatera Utara, Medan 20155, Indonesia
Corresponding author: suratniafrianti@unprimdn.ac.id

Article info

Article history:
Received 17 September 2026
Revised 18 October 2026
Accepted 22 October 2026
Available online xxx

E–ISSN:
P–ISSN:

How to cite:
S. Afrianti, A. A. Tarigan, T. B. Nur, "Integrated Aspen Plus Simulation of Biogas Upgrading and Electricity Generation from Palm Oil Mill Effluent," Eco Chemical Engineering Journal, Vol. 1 No. 1.

This work is licensed under a Creative Commons Attribution–ShareAlike 4.0 International.
http://doi.org/10.26594/register.v6i1.idarticle

Abstract

Palm oil mill effluent (POME) offers an opportunity to combine wastewater mitigation with renewable-energy recovery. This study evaluates an integrated steady-state Aspen Plus V11 POME-to-power simulation comprising feed cooling, stoichiometric anaerobic digestion, five-stage water scrubbing, air addition, gas-liquid separation, compression, and turbine-based power conversion. At the reported POME feed rate of 900 m^3h^{-1} at 70 °C and 1 atm, the feed was cooled to 33 °C before digestion at 2.5 atm. The digester produced gas containing 61.2% CH_4, 34.0% CO_2, 2.0% H_2S, 0.4% NH_3, and 1.8% H_2O. Five-stage water scrubbing increased CH_4 to 70.0% and reduced H_2S to 0.25%; after conditioning, the final gas contained 71.0% CH_4, 26.0% CO_2, 1.36% O_2, and 0.25% H_2S. The power block generated 837.5 kW, equivalent to an indicative gross output of 0.93 kWh per m^3 of POME. Relative methane enrichment from digester gas to final gas was 16.0%, while the reported H_2S fraction decreased by 87.5% across the scrubber. The integrated configuration demonstrates the technical potential of POME-to-power conversion, but feed and stream closure, methane-slip quantification, scrubber optimization, model validation, and complete net-energy accounting remain necessary before plant-scale application.

Keywords: Palm oil mill effluent, Biogas, Aspen Plus, Gas upgrading, Methane

1. Introduction

Palm oil mill effluent (POME) is one of the largest liquid by-products generated during crude palm oil processing. Its high biochemical and chemical oxygen demand can create a substantial pollution burden when the effluent is treated only in open ponds or discharged without adequate stabilization. At the same time, its biodegradable organic content makes POME a valuable substrate for anaerobic digestion and renewable-energy recovery. Recent assessments emphasize that converting POME into biogas can reduce wastewater impacts, mitigate uncontrolled methane emissions, and create useful energy within a circular-bioeconomy framework [1], [2].

Anaerobic digestion converts complex organic matter through hydrolysis, acidogenesis, acetogenesis, and methanogenesis. The resulting biogas is dominated by methane (CH_4) and carbon dioxide (CO_2), with smaller amounts of hydrogen sulfide (H_2S), ammonia (NH_3), water vapor, and other trace components. Pilot-scale work in Indonesia has demonstrated the technical feasibility of POME-to-biogas conversion, while full-scale evaluations show that captured POME biogas can support electricity generation and greenhouse-gas mitigation [3], [4]. However, CO_2 lowers the fuel value, H_2S is corrosive and toxic, and excess water can impair downstream equipment, making gas cleaning and upgrading important before compression and energy conversion [5], [6].

Water scrubbing is attractive for POME-derived biogas because CO_2 and H_2S are more soluble in water than CH_4 and the process avoids direct use of reactive chemical solvents. Aspen-based studies show that

methane purity and recovery depend strongly on pressure, water flow rate, temperature, and stage number [5], [7]. Process simulation therefore provides a useful framework for integrating digestion, gas purification, and power conversion before pilot- or plant-scale implementation. Previous POME simulations have also demonstrated the value of flowsheet modelling for linking treatment, upgrading, and energy recovery [8], [9]. In the present configuration, the NRTL property method was selected for the source model.

The objective of this study was to consolidate and evaluate the reported Aspen Plus V11 POME-to-power simulation as an integrated process. The analysis focuses on: (i) the simulation basis, feed representation, and stoichiometric digestion model; (ii) changes in major and minor biogas components through purification and conditioning; (iii) the reported electricity output on a POME-feed basis; and (iv) engineering limitations and optimization opportunities relevant to future plant-scale application. Derived indicators are restricted to calculations supported directly by the reported stream values, without inventing or normalizing unreported data.

2. Method

2.1. Simulation basis and POME feed

The process was modeled as a steady-state flowsheet in Aspen Plus V11. The simulated train consisted of a POME feed pump, cooler, stoichiometric anaerobic digester, five-stage water scrubber, mixer for air addition, water trap, compressor, and turbine-based power-conversion block. The reported POME feed rate was 900 m^3h^{-1} at 70 °C and 1 atm. Before digestion, the feed was pressurized and cooled to 33 °C, while the digester operated at 33 °C and 2.5 atm. Table 1 shows physicochemical characteristics of POME digestion process. The Non Random Two Liquid (NRTL) property method was used in the source model for phase-equilibrium calculations involving aqueous and gas streams. Because the original Aspen Plus model file was not available, the present work treats the reported simulator outputs as the primary numerical record and does not independently reconstruct unreported model inputs.

Table 1. Physicochemical characteristics of POME used in the study.

Parameter	Concentration range
Chemical oxygen demand (mg L^{-1})	15,000–100,000
Biochemical oxygen demand (mg L^{-1})	10,250–43,750
Total solids (mg L^{-1})	11,500–79,000
Total suspended solids (mg L^{-1})	5,000–54,000
Oil and grease (mg L^{-1})	130–18,000
Temperature (°C)	80–90
pH	3.4–5.2

For the Aspen feed representation, the source reports component fractions of 0.002 n-hexadecanoic acid, 0.002 stearic acid, 0.002 n-tetradecanoic acid, 0.002 oleic acid, 0.020 linoleic acid, 0.950 water, and 0.040 protein. These values sum to 1.018 rather than exactly 1.000. Because the underlying Aspen input file was not supplied, the reported fractions are retained without re-normalization; the discrepancy is treated as a model-reporting limitation rather than corrected by assumption.

2.2. Stoichiometric anaerobic digestion

Anaerobic digestion was represented by stoichiometric conversion of major fatty-acid and protein surrogate components at 33 °C and 2.5 atm. The reaction set used in the source model is reproduced below because it defines the basis of the simulated digester products:

$$2C_{16}H_{32}O_2 + 14H_2O \rightarrow 23CH_4 + 9CO_2 \quad (1)$$

$$C_{18}H_{36}O_2 + 8H_2O \rightarrow 13CH_4 + 5CO_2 \quad (2)$$

$$C_{14}H_{28}O_2 + 6H_2O \rightarrow 10CH_4 + 4CO_2 \quad (3)$$

$$5C_{18}H_{34}O_2 + 34H_2O \rightarrow 51CH_4 + 21CO_2 \quad (4)$$

$$2C_{18}H_{32}O_2 + 18H_2O \rightarrow 25CH_4 + 11CO_2 \quad (5)$$

$$2C_{13}H_{25}O_7N_3S + 12H_2O \rightarrow 13CH_4 + 13CO_2 + 6NH_3 + 2H_2S \quad (6)$$

This stoichiometric approach provides a transparent estimate of product-gas composition from simplified feed surrogates, but it does not explicitly resolve microbial kinetics, hydraulic retention time, organic loading rate, inhibition, or COD destruction. Consequently, the digester is best interpreted as a process-design representation rather than a dynamic biological model. Industrial-scale studies indicate that retention time and recycle conditions can materially affect methane yield and should be optimized when moving from conceptual simulation to plant operation [10].

2.3. Biogas purification and conditioning

Table 2 shows principal operating conditions used in the integrated Aspen Plus simulation. Raw biogas from the digester was purified in a five-stage scrubber without a condenser or reboiler. Water entered the top of the column at 600 m^3 h^{-1}, 30 °C, and 2.5 atm, while the scrubber stages were reported at 1.5 atm; the gas entered from the lower stage and contacted the water counter-currently. Water scrubbing exploits the greater aqueous solubility of CO_2 and H_2S relative to CH_4, although industrial systems commonly use higher pressure to increase the absorption driving force [6], [11]. Downstream, the scrubbed gas was mixed with air at 300 m^3 h^{-1}, 28 °C, and 1.2 atm. A water trap at 30 °C and 4 atm separated residual liquid before compression and power conversion. Reconstructed process sequence and operating conditions from the reported Aspen Plus simulation is shown in Figure 1.

Table 2. Operating conditions used in the Aspen Plus simulation.

Unit operation	Key reported condition	Temperature	Pressure
POME feed	900 m^3 h^{-1}	70 °C	1 atm
Cooler outlet	Cooled POME	33 °C	2.5 atm
Anaerobic digester	Stoichiometric model	33 °C	2.5 atm
Water scrubber	5 stages; water 600 m^3 h^{-1}	30 °C solvent	1.5 atm stages
Air mixer	Air 300 m^3 h^{-1}	28 °C	1.2 atm
Water trap	Gas-liquid separation	30 °C	4 atm
Compressor	15 kW; η_{is} = 72%	-	-
Power block	η_{is} = 72%; 837.5 kW	-	1 atm outlet

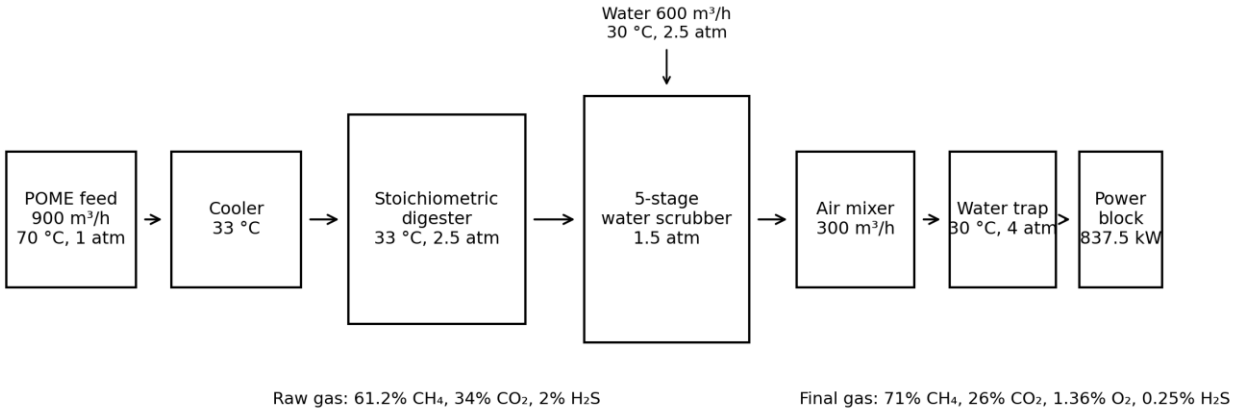


Figure 1. Process sequence and operating conditions in Aspen Plus simulation.

2.4. Compression, power conversion, and data treatment

The conditioned gas was compressed using an Aspen compressor block reported at 15 kW with an isentropic efficiency of 72%. The final power-conversion step was represented by a turbine block operating at a reported isentropic efficiency of 72% and discharging at 1 atm. Although the source narrative occasionally refers to a gas engine, the flowsheet and reported results use a turbine-based power block; the modeled unit is therefore described here as the turbine or power-conversion block. The reported gross electrical output was 837.5 kW. All stream compositions and flow rates were otherwise retained as reported. Because several gas

compositions do not sum exactly to 100% and the flow-rate basis changes between some unit operations, no mass-balance correction or component-recovery calculation was imposed. Relative changes below therefore refer to the reported component fractions rather than rigorously closed recovery efficiencies.

$$Methane\ enrichment(\%) = \frac{X_{final\ methane} - X_{digester\ methane}}{X_{digester\ methane}} \quad 7)$$

and

$$Gross\ specific\ electrical\ output = \frac{P_e}{Q_{POME}} \quad 8)$$

Where: $X_{methane}$ is the methane fraction,
P_e is the gross electrical power (kW), and
Q_{POME} is the POME feed rate ($m^3\ h^{-1}$).

The resulting specific output has units of kWh per m^3 of POME under the steady-state interpretation and does not represent net plant efficiency because pumping, cooling, scrubber-water circulation, compression, and other auxiliary loads are not completely reported.

3. Results and Discussion

3.1. Raw biogas from the stoichiometric digester

The digester produced a reported gas composition of 61.2% CH_4, 34.0% CO_2, 2.0% H_2S, 0.4% NH_3, and 1.8% H_2O, at a reported gas flow rate of 17,933.8 m^3h^{-1}. A methane fraction of approximately 60% is broadly consistent with anaerobic digestion of high-strength organic waste and with POME biogas used for electricity generation [2], [4], providing a plausible qualitative basis for downstream upgrading. The corresponding liquid effluent was reported to contain approximately 92% water, 3% protein, 0.18% acid compounds, and smaller quantities of dissolved or entrained gases. Because the model uses simplified surrogate components and was not calibrated against COD removal, volatile-solids destruction, or methane yield per unit of COD removed, these outputs should be interpreted as model stream estimates rather than validated digester performance. Plant-scale validation should include these biological performance indicators [8], [10].

3.2. Effect of water scrubbing on biogas composition

After the five-stage water scrubber, the reported CH_4 fraction increased from 61.2% to 70.0%, while CO_2 decreased from 34.0% to 25.0%, H_2S decreased from 2.0% to 0.25%, and NH_3 was reported as 0%. H_2O increased from 1.8% to 2.8%. Figure 2 shows reported CH_4 and CO_2 fractions across the simulated gas-treatment train. On a reported-composition basis, methane increased by 8.8 percentage points, equivalent to a 14.4% relative increase from the digester-gas value, while the H_2S fraction decreased by 87.5%. The directional changes are consistent with preferential absorption of acid-gas components in water.

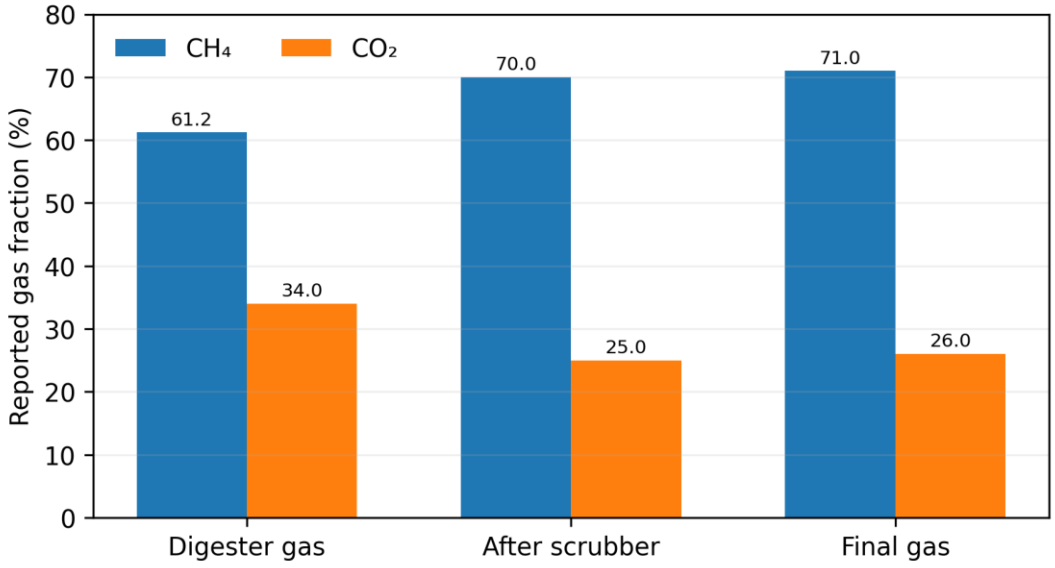


Figure 2. Methane and CO_2 fractions across the simulated gas-treatment train.

The source reports a scrubbed-gas flow rate of 23,735.3 $m^3\ h^{-1}$ and a scrubber-bottom flow rate of 613.4 m^3h-1. Because the reported gas flow after scrubbing is higher than the digester-gas flow and the available stream basis is insufficient to reconcile this increase, methane recovery, solvent loading, and overall mass-balance closure cannot be inferred reliably from these values.

The degree of methane enrichment is moderate relative to optimized high-pressure water-scrubbing systems. An Aspen Plus optimization study reported methane purity up to 99.3% after adjusting pressure, temperature, water flow rate, and stage number [7]. Reviews likewise indicate that water scrubbing benefits from elevated pressure because CO_2 and H_2S absorption increases with pressure [6], [11]. The reported 1.5 atm stage pressure therefore represents an important optimization opportunity. Increasing pressure, adjusting the water-to-gas ratio, adding stages, or introducing water regeneration could raise methane purity, although these changes would also increase compression duty and process complexity.

The scrubber-bottom stream was reported to be predominantly water with smaller fractions of CH_4, CO_2, NH_3, and H_2S. This indicates a need to quantify methane slip: methane dissolved in scrubbing water represents both an energy loss and a potential greenhouse-gas emission if the solvent is depressurized without recovery. Energy and exergy analyses show that high methane recovery requires an appropriately designed pressure and flash-recovery scheme [12].

3.3. Final gas conditioning

Air addition and subsequent liquid separation changed the reported final gas composition to 71.0% CH_4, 26.0% CO_2, 1.36% O_2, and 0.25% H_2S. Relative to digester gas, methane increased by 9.8 percentage points, corresponding to a 16.0% relative enrichment. The final H_2S fraction remained at 0.25%, indicating that the water trap primarily served as a gas-liquid separation step rather than an additional sulphur-removal step. Final NH_3 and H_2O fractions were not reported and are therefore not inferred. Reported minor gas components across the simulated process is shown in Figure 3. Missing final NH_3 and H_2O values were not inferred.

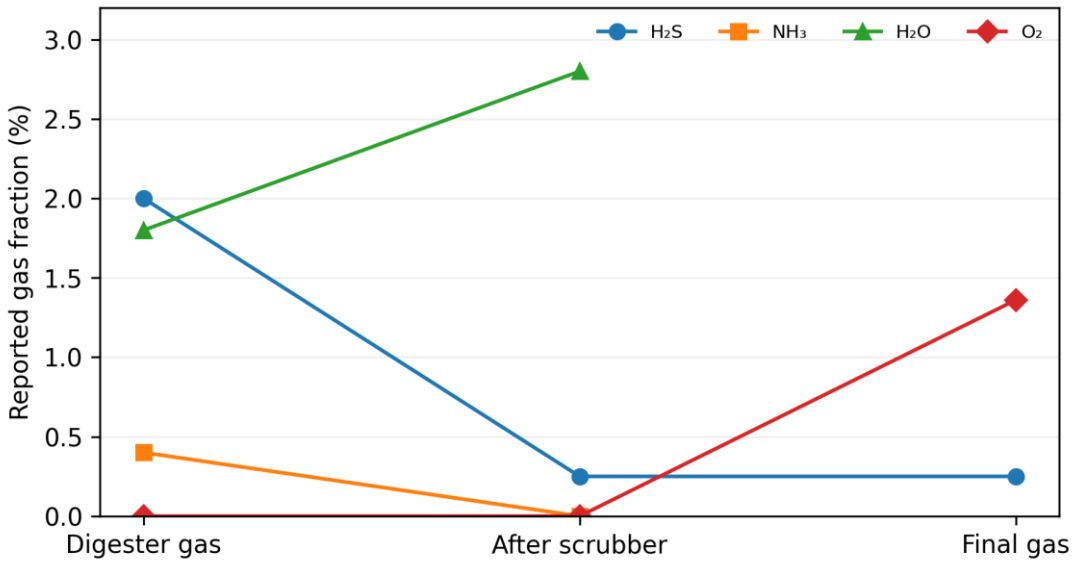


Figure 3. Minor gas components across the simulated process.

Table 3. Gas composition through the upgrading train.

Stream	CH_4 (%)	CO_2 (%)	H_2S (%)	NH_3 (%)	H_2O (%)	O_2 (%)
Digester gas	61.2	34.0	2.0	0.4	1.8	0
After scrubber	70.0	25.0	0.25	0	2.8	0
Final gas	71.0	26.0	0.25	not reported	not reported	1.36

Table 3 reported gas composition through the upgrading train. For real power-generation equipment, residual H_2S and moisture should be checked against manufacturer fuel-gas specifications because sulphur compounds and condensate can cause corrosion, deposits, and accelerated maintenance. The modelled air-addition step also warrants detailed safety review. In industrial combustion systems, oxidant is normally

controlled at the combustor or engine intake rather than premixed with methane-rich fuel far upstream, because oxygen-containing fuel mixtures can create flammability constraints. The Aspen sequence should therefore be treated as a simulation simplification requiring revision during detailed design.

3.4. Electricity generation and process level interpretation

The power-conversion block generated a reported 837.5 kW at a turbine isentropic efficiency of 72%. The source abstract expresses this result as 837.5 kWh^{-1}our, whereas the conclusion reports 837.5 kW. Because electrical power is a rate quantity, the value is reported here as 837.5 kW while the source-unit inconsistency is retained as a documentation limitation. The compressor duty was reported as 15 kW, but a complete plant auxiliary-load balance was not provided.

Using the reported POME feed rate of 900 m^3h^{-1}, the gross power corresponds to approximately 0.93 kWh per m^3 of POME. This is an indicative gross metric only and should not be interpreted as net plant efficiency. A complete assessment would require the electrical demand of pumping, feed cooling, scrubber-water circulation, compression, and other auxiliaries, together with a consistent fuel-energy balance for the conditioned gas. Nevertheless, field evaluation in Indonesia and previous process studies support the broader technical premise that POME biogas can contribute materially to palm-oil-mill electricity demand [4], [9].

The simulation demonstrates an integrated pathway in which POME is converted to methane-containing biogas, upgraded through water scrubbing, conditioned for combustion, and used for power generation. However, the reported feed fractions sum to 1.018, several gas compositions do not close exactly to 100%, and the reported flow-rate changes between major units cannot be fully reconciled from the manuscript alone. These inconsistencies do not invalidate the flowsheet concept, but they limit quantitative claims regarding component recovery, conversion efficiency, and net energy efficiency.

3.5. Comparison with recent process simulation literature

The simulated methane enrichment to 70–71% is lower than the purity achievable in optimized biomethane systems, but it clearly illustrates how gas cleaning can improve fuel quality relative to raw POME biogas. In a water-scrubber optimization study, methane purity reached 99.3% after optimization of pressure, temperature, water flow rate, and stage number [7]. The present flowsheet is therefore better interpreted as an integrated proof-of-concept for POME-to-power than as an optimized biomethane-upgrading design.

Recent work has increasingly emphasized industrial-scale optimization, validation against operating plants, and techno-economic assessment. Full-scale POME treatment simulations have demonstrated the importance of combining process modelling with cost optimization [8], while industrial-scale studies show that hydraulic retention time and recycle conditions can strongly affect biogas yield [10]. For Indonesian deployment, techno-economic evidence further indicates that POME-to-power systems can reduce greenhouse-gas emissions but remain sensitive to feed availability, technology configuration, and project economics [4]. These studies point to validation and optimization as the most important next steps for the current Aspen model.

3.6. Model limitations and future development

Several limitations should be addressed before the simulation is used for equipment design or investment decisions. First, the POME component fractions do not close exactly to unity and several gas compositions do not close exactly to 100%. Second, the reported gas-flow basis changes across the scrubber in a way that cannot be independently reconciled without the original Aspen file and a complete stream table. Third, the stoichiometric digester does not represent biological kinetics, COD removal, hydraulic retention time, or inhibition. Fourth, the NRTL property method should be benchmarked against alternative thermodynamic formulations for gas-rich sections. Fifth, gross turbine output is reported without a complete auxiliary-power balance, and the narrative reference to a gas engine should be reconciled with the turbine block shown in the simulation.

Future development should include: (i) normalization and closure of feed and product streams; (ii) calibration of digestion against measured COD removal and methane yield; (iii) optimization of scrubber pressure, water flow, temperature, and stage number; (iv) methane-slip recovery and water-recycle modeling; (v) explicit combustion modeling with equipment-specific gas-quality and safety limits; (vi) gross and net electrical-efficiency calculations; and (vii) techno-economic and life-cycle assessment. These additions would move the current proof-of-concept toward a decision-grade model for industrial POME valorization.

4. Conclusion

An integrated Aspen Plus V11 simulation was evaluated for conversion of palm oil mill effluent to electricity through feed cooling, stoichiometric anaerobic digestion, five-stage water scrubbing, gas conditioning, compression, and a turbine-based power block. The reported digester gas contained 61.2% CH_4 and 34.0% CO_2. Water scrubbing increased CH_4 to 70.0% while reducing H_2S from 2.0% to 0.25%; after conditioning, the final gas contained 71.0% CH_4, 26.0% CO_2, 1.36% O_2, and 0.25% H_2S. The reported gross power output was 837.5 kW, corresponding to approximately 0.93 kWh per m^3 of POME at the reported feed rate. Relative methane enrichment from digester gas to final gas was 16.0%, and the reported H_2S fraction decreased by 87.5% across the scrubber. The combined evidence supports the technical potential of integrated POME-to-power conversion but also shows that the current configuration is not yet an optimized or fully validated plant model. Mass-balance closure, biological calibration, higher-performance gas upgrading, methane-slip recovery, explicit combustion and safety assessment, and complete net-energy and techno-economic evaluation are required before industrial performance can be established.

Acknowledgements

The authors gratefully acknowledge the Laboratory of Ecology, Universitas Sumatera Utara, for supporting the research.

Declaration of AI Use

During the preparation of this article, the authors used Grammarly for improving grammar and enhancing the clarity and structure of English sentences.

References

[1] M. N. I. Salehmin, S. K. Tiong, H. Mohamed, B. S. Zainal, S. S. Lim, N. H. M. Yasin, and Z. Zakaria, "Sustainable bioenergy from palm oil mill effluent: Advancements in upstream and downstream engineering with techno-economic and environmental assessment," *Journal of Industrial and Engineering Chemistry*, vol. 133, pp. 122-147, 2024, doi: 10.1016/j.jiec.2023.12.033.

[2] A. B. Nasrin, A. A. Abdul Raman, N. A. Bukhari, M. A. Sukiran, A. Buthiyappan, V. Subramaniam, A. Abdul Aziz, and S. K. Loh, "A critical analysis on biogas production and utilisation potential from palm oil mill effluent," *Journal of Cleaner Production*, vol. 361, art. 132040, 2022, doi: 10.1016/j.jclepro.2022.132040.

[3] Irvan, B. Trisakti, S. Maulina, and H. Daimon, "Production of biogas from palm oil mill effluent: From laboratory scale to pilot scale," *Rasayan Journal of Chemistry*, vol. 11, no. 1, pp. 378-385, 2018, doi: 10.7324/RJC.2018.1112028.

[4] A. Sodri and F. E. Septriana, "Biogas Power Generation from Palm Oil Mill Effluent (POME): Techno-Economic and Environmental Impact Evaluation," *Energies*, vol. 15, no. 19, art. 7265, 2022, doi: 10.3390/en15197265.

[5] M. U. Khan, J. T. E. Lee, M. A. Bashir, P. D. Dissanayake, Y. S. Ok, Y. W. Tong, M. A. Shariati, S. Wu, and B. K. Ahring, "Current status of biogas upgrading for direct biomethane use: A review," *Renewable and Sustainable Energy Reviews*, vol. 149, art. 111343, 2021, doi: 10.1016/j.rser.2021.111343.

[6] O. A. Aworanti, A. O. Ajani, O. O. Agbede, S. E. Agarry, O. Ogunkunle, O. T. Laseinde, M. A. Kalam, and I. M. R. Fattah, "Enhancing and upgrading biogas and biomethane production in anaerobic digestion: A comprehensive review," *Frontiers in Energy Research*, vol. 11, art. 1170133, 2023, doi: 10.3389/fenrg.2023.1170133.

[7] T. L. K. Law, Y. A. Dahawi, S. N. Abdul Rahman, and A. Abdulrazik, "Simulation and optimisation for production of biogas from palm oil mill effluent (POME) using Aspen Plus," *International Journal of Biomass and Renewables*, vol. 10, no. 2, pp. 9-17, 2021.

[8] X. Lok, Y. J. Chan, and D. C. Y. Foo, "Simulation and optimisation of full-scale palm oil mill effluent (POME) treatment plant with biogas production," *Journal of Water Process Engineering*, vol. 38, art. 101558, 2020, doi: 10.1016/j.jwpe.2020.101558.

[9] S. E. Hosseini and M. A. Wahid, "Utilization of biogas released from palm oil mill effluent for power generation using self-preheated reactor," *Energy Conversion and Management*, vol. 105, pp. 957-966, 2015, doi: 10.1016/j.enconman.2015.08.058.

[10] K. W. Kan, Y. J. Chan, T. J. Tiong, and J. W. Lim, "Maximizing biogas yield from palm oil mill effluent (POME) through advanced simulation and optimisation techniques on an industrial scale," *Chemical Engineering Science*, vol. 285, art. 119644, 2024, doi: 10.1016/j.ces.2023.119644.

[11] H. Karne, U. Mahajan, U. Ketkar, A. Kohade, P. Khadilkar, and A. Mishra, "A review on biogas upgradation systems," *Materials Today: Proceedings*, vol. 72, part 3, pp. 775-786, 2023, doi: 10.1016/j.matpr.2022.09.015.

[12] G. Vilardi, C. Bassano, P. Deiana, and N. Verdone, "Exergy and energy analysis of three biogas upgrading processes," *Energy Conversion and Management*, vol. 224, art. 113323, 2020, doi: 10.1016/j.enconman.2020.113323.